

Novel Benzothiazole based Highly Selective Ratiometric Fluorescent *turn on* Sensor for Zn²⁺ and Colorimetric Chemosensor for Zn²⁺, Cu²⁺ and Ni²⁺ Ions

Chinna Ayya Swamy Pothulapadu^{a*}, Anjitha Jayaraj^a, Swathi N^b, Ragam N Priyanka^c and
Gandhi Sivaraman^d

^aMain group Organometallics Materials, Supramolecular Chemistry and Catalysis lab,
Department of Chemistry, National Institute of Technology, Calicut, India-673601.

^bMaharani Lakshmi Ammanni College for women (autonomous), Bangalore, India-560012

^cSchool of Chemical Sciences, Mahatma Gandhi University, Kottayam, India-686560.

^dDepartment of Chemistry, Gandhigram Rural Institute (Deemed to be University),
Gandhigram 624302, India

Table of contents for supporting information	Page number
1. Methods and Materials	S2-S4
2. Photophysical Properties	S5-S9
3. ¹ H and ¹³ C Nuclear Magnetic Resonance (NMR) and High-Resolution Mass Spectroscopic (HRMS) studies	S10-S12
4. Density Functional Theory results	S13-S25

1. Methods and Materials

1.1 UV-visible and fluorescence titration

UV-Visible and fluorescence titration of **compound-1** was carried out in 1:1 mixture of CHCl₃ and DMSO solutions. **Compound-1** (1 mL, 1 × 10⁻⁵ M) were placed in a cuvette and was titrated with incremental amount of metal ion (1×10⁻³ M) solution in 1:1 mixture of CHCl₃ and DMSO solutions.

1.2 Details about the association constant^{1,2}

For compound Compound-1:

Chloroform solution of compounds **compound-1** (1 mL, 1 × 10⁻⁵ M) were placed in a cuvette and was titrated with incremental amount of metal ions (1×10⁻³ M) solution in 1:1 ratio of H₂O and DMSO. The changes associated with the absorption band at 410 nm were monitored. The calculation for compound **compound-1** is shown below.



$$I = k_s[\text{compound-1}] + k_p[\text{compound-1} \cdot [\text{Metal}]^2]$$

$$I_0 = k_s[\text{compound-1}]_0$$

$$[\text{compound-1}]_0 = [\text{compound-1}] + [\text{compound-1} \cdot [\text{Metal}]^2]$$

$$K = [\text{compound-1} \cdot [\text{Metal}]^2] / [\text{compound-1}] [\text{Metal}]^2 \quad (K \text{ is association constant})$$

$$\begin{aligned} I/I_0 &= (k_s[\text{compound-1}] + k_p[[\text{Metal ion}]^2 \cdot \text{compound-1}]) / k_s[\text{compound-1}]_0 \\ &= (k_s[\text{compound-1}] + k_p[[\text{Metal ion}]^2 \cdot \text{compound-1}]) / k_s ([\text{compound-1}] + [\text{Metal ion} \cdot \text{compound-1}]) \end{aligned}$$

$$I/I_0 = (1 + (k_p/k_s) K[\text{Metal}]^2) / (1 + K[\text{Metal}]^2) \quad (1 - I/I_0) / [\text{Metal}]$$

$$k_p/k_s = \alpha \quad (\text{constant})$$

$$I/I_0 = (1 + \alpha K[\text{Metal}]^2) / (1 + K[\text{Metal}]^2)$$

$$1-I/I_0 = 1-(1+ \alpha K[\text{Metal}]^2) / (1+K[\text{Metal}]^2)$$

$$= (1+K[\text{Metal}]^2-1- \alpha K[\text{Metal}]) / (1+K[\text{Metal}]^2)$$

$$= (K[\text{Metal}]^2- \alpha K[\text{Metal}]) / (1+K[\text{Metal}]^2)$$

$$(1-I/I_0)*(1+K[\text{Metal}]^2) = K[\text{Metal}]^2- \alpha K[\text{Metal}]^2$$

$$(1-I/I_0) = K[\text{Metal}]^2 (I/I_0)- \alpha K[\text{Metal}]^2$$

$$(1-I/I_0)/ [\text{Metal}]^2 = K(I/I_0)- \alpha K$$

Here, I_0 is initial absorbance of respective band, I is absorbance of respective band I upon addition of eqve of metal ions.

The association constant is obtained from the slope of $(1 - I/I_0)/ [\text{Metal}]^2$ Vs I/I_0 and are given in Table S1 (Figure 9).

$A = \epsilon Cl$, here ϵ = molar extension constant, C = concentration of sample, l = path length

$$= \epsilon l [C]$$

$$= K_s [C] \text{ for substrate}$$

$$= K_p [C] \text{ for product}$$

1.3 Calculation of Detection Limit

The detection limit was calculated from the fluorescence quenching titration experiment. The intercept to X-axis (here $\log[\text{metal}]$) was obtained by linear fitting of the $(I_{\text{max}}-I)/(I_{\text{max}}-I_{\text{min}})$ vs $\log[\text{metal}]$, where I_{max} , I and I_{min} are the initial fluorescence intensity, intensity at particular concentration and intensity at saturation point respectively. The detection limits were calculated by the formula, $([\text{metal}] \times \text{MW of metal ions})/1000$ (multiplied by 10^6 to get the values in ppm), where MW [metal] is the molecular weight of metal.

1.4 Fluorescence quenching titration study:

The fluorescence quenching experiments were carried in 1:1 ratio of CHCl_3 and DMSO. The stock solution of **compound-1** is 1×10^{-5} M placing 1 mL quartz cuvette and followed metal ions 1×10^{-3} M were added gradually increasing amount. For each addition, at least three fluorescence spectrums were recorded repeatedly at 298 K to obtain a concordant value. **compound-1** were excited at 375 nm and the emission was monitored at 575 nm, whereas slit

width was kept 2 nm both source and detector through the experiment. Fluorescence quenching efficiency for each analyte was calculated by the following equation,

$$\eta = (I_0 - I) / I_0 \times 100\%$$

where, I_0 is the initial intensity of the **Compound-1** and I is the intensity after the addition of a fixed volume of analytes.

Stern-Volmer constants (K_{SV}) were obtained for both cases, **compound-1**, from I_0/I vs [metal ions] plots by fitting using Stern-Volmer equation,

$$I_0/I = 1 + K_{SV}[\text{metal ions}]$$

1.5 Fluorescence quantum yield

The fluorescence quantum yield of molecules can be determined as the ratio of number of the photons emitted to the number of photons that are absorbed. The quantum yield of an ideal molecule is 1.0, which is the maximum efficiency. The quantum efficiency can be calculated by using the acute luminescence of standard sample whose emission or absorption spectrum falls in the region of the unknown compounds. The quantum efficiency of an unknown sample can be determined from the comparison of absorbance and emission area of standard sample with unknown compound, using the standard equation 1.

$$\phi_u = [(A_s F_u n_u^2) / (A_u F_s n_s^2)] \phi_s \quad (1)$$

Here the subscript u stands for unknown, s stands for known and ϕ is quantum efficiency, A_s stands for absorbance of standard, A_u is the absorbance of unknown, F_s stands for integrated emission of standard, F_u is integrated emission of unknown and n is the refractive index of solvents used. Generally, absorbance of a standard and unknown sample should be similar or small which is around 0.1. Maximum quantum yield (Φ) of compounds, can be achieved either by designing a material with a rapid rate of radiative decay, or by minimizing competing nonradiative processes.

2. Photophysical Properties

Table S1: Photophysical data of **compound-1-1**, **S compound-1+Zn²⁺**, **compound-1+ Ni²⁺**, **compound-1+Cu²⁺** ions,

	compound-1	compound-1-Zn²⁺	compound-1-Ni²⁺	compound-1-Cu²⁺
Association constant, K _a		4.9 x 10 ¹¹	1.6 x 10 ¹¹	6.0 x 10 ¹⁰
Quantum yield ^a , ^b	0.55	0.69	0.07	0.05
Quenching constant ^c		2.0 x 10 ⁵	5.6 x 10 ⁵	2.4 x 10 ⁵
Quenching efficiency ^d		69%	98%	96%

b) Quantum yields are calculated using quinine sulphate (0.1 M in H₂SO₄, Φ_F = 57.7%) solution as reference and using the following formula $\Phi = \Phi_F \times I/I_R \times A_R/A \times \eta^2 / \eta R^2$ where Φ = quantum yield, I = intensity of emission, A = absorbance at λ_{ex}, η = refractive index of solvent.

c) The quantum yields of compounds are determined in a 1:1 ratio of DMSO and CHCl₃ and the standard error is equal to the standard deviation of five independent measurements.

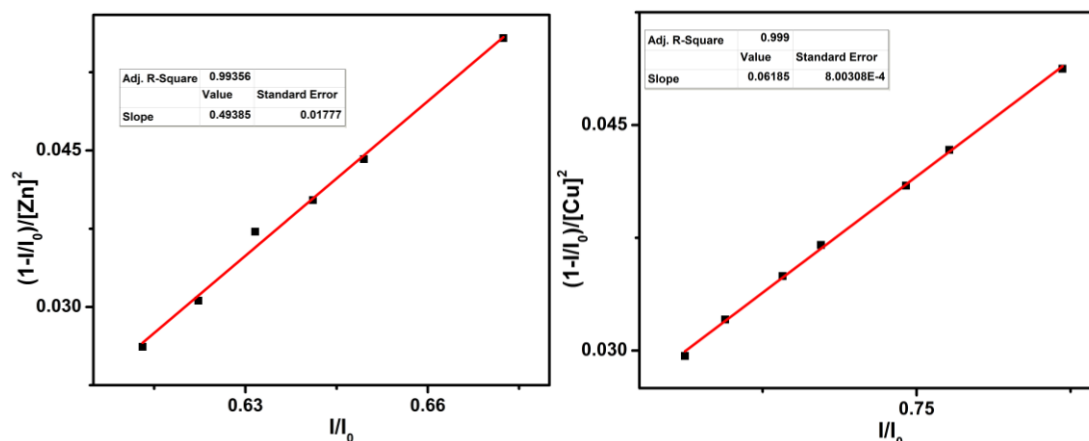


Figure S1: The I/I_0 vs $(1 - I/I_0)/[Metal]²$ plot for absorption titration data of **compound-1** with Zn²⁺ (left) and Cu²⁺ (right) ions in 1:1 ratio of DMSO and CHCl₃

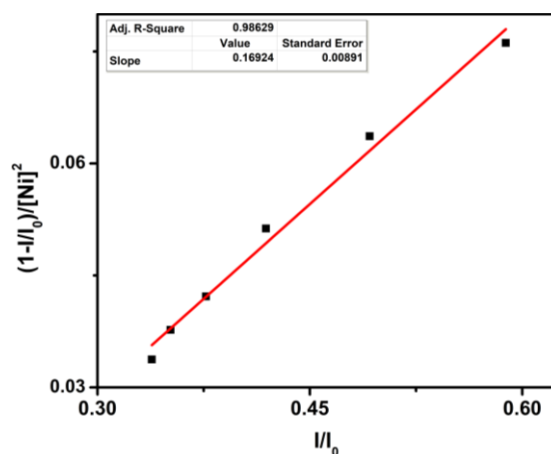


Figure S2: The I/I_0 vs $(1 - I/I_0)/[\text{Metal}]^2$ plot for absorption titration data of **compound-1** with Ni^{2+} ions in 1:1 ratio of DMSO and CHCl_3

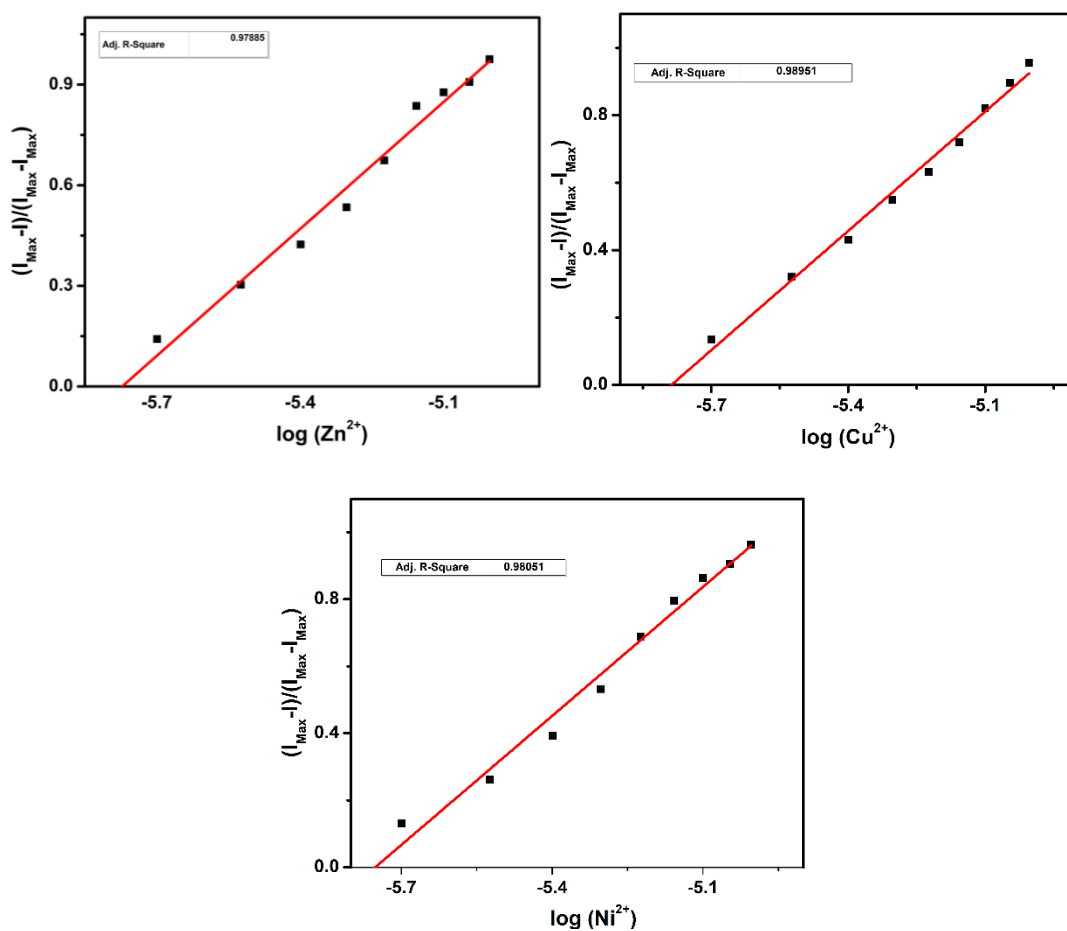


Figure S3: $(I_{\text{max}} - I)/(I_{\text{max}} - I_{\text{min}})$ vs $\log[\text{metal ions}]$ plots for **compound-1** with Zn^{2+} (top left), Cu^{2+} (top right) and Ni^{2+} (bottom) ions in 1:1 ratio of DMSO and CHCl_3

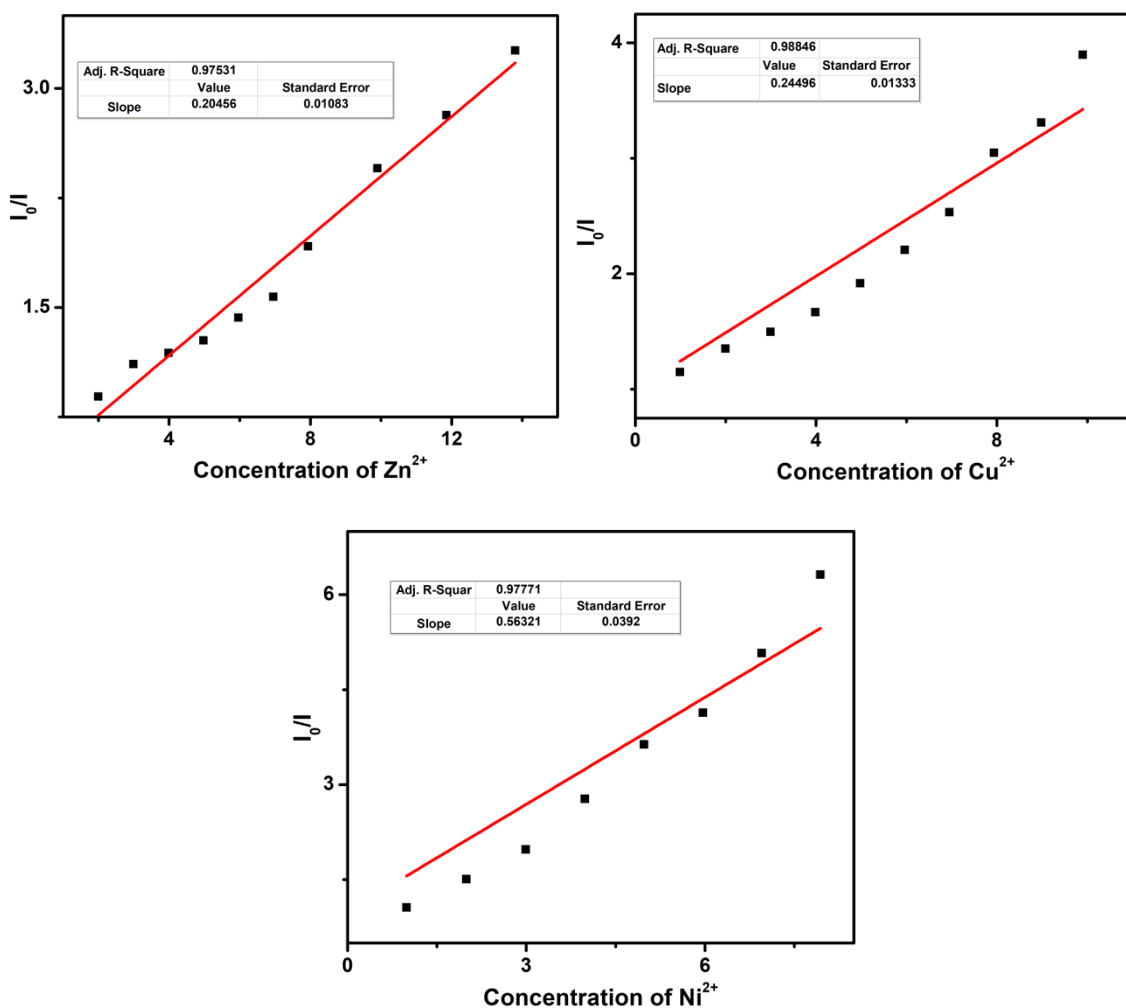


Figure S4: Stern-Volmer plots for **compound-1** with Zn²⁺ (top left), Cu²⁺ (top right) and Ni²⁺ (bottom) ions in 1:1 ratio of DMSO and CHCl₃

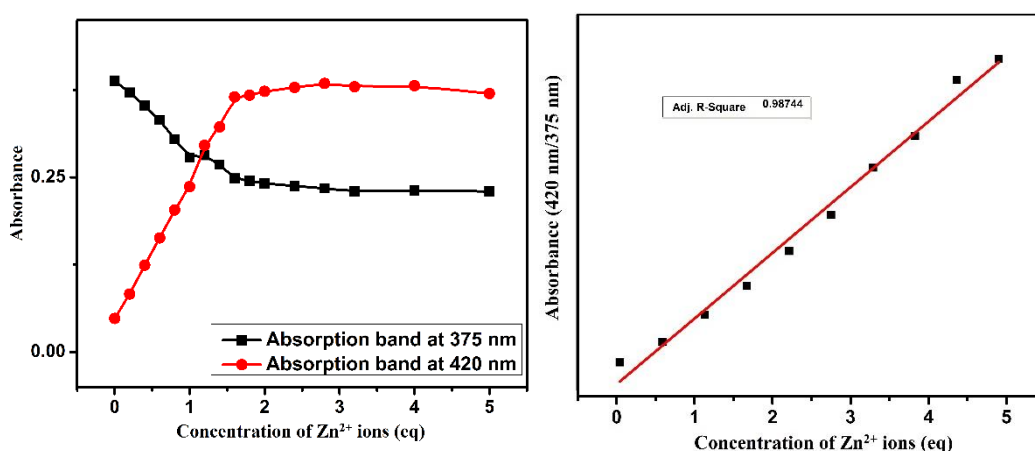


Figure S5: The compared absorption bands at 375 nm and 420 nm, which indicates the ratiometric response towards Zn²⁺ ions (left) and linear fitting between the ratio of 420 nm/375 nm absorption bands and upon incremental of concentration of Zn²⁺ ions

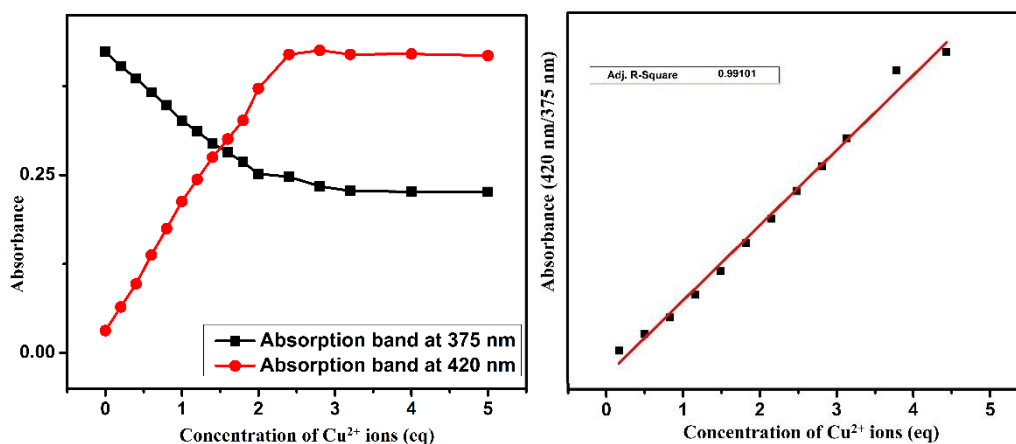


Figure S6: The compared absorption bands at 375 nm and 420 nm, which indicates the ratiometric response towards Cu²⁺ ions (left) and linear fitting between the ratio of 420 nm/375 nm absorption bands and upon incremental of concentration of Cu²⁺ ions

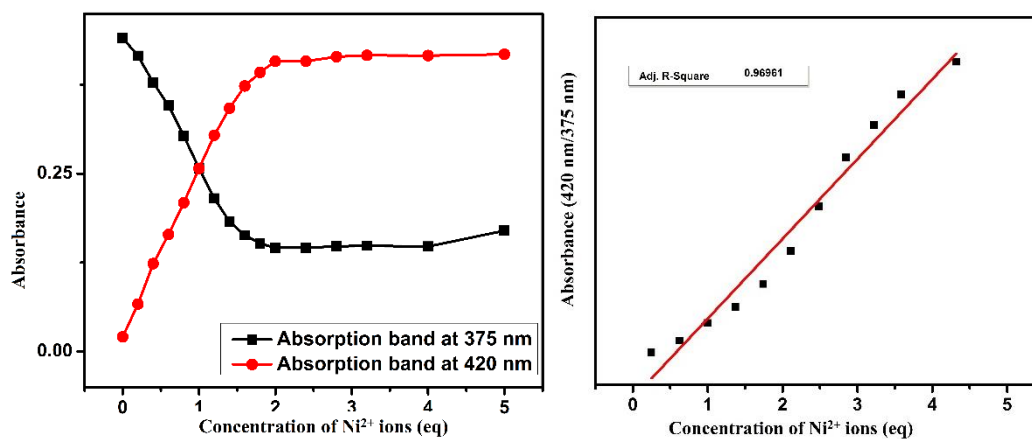


Figure S7: The compared absorption bands at 375 nm and 420 nm, which indicates the ratiometric response towards Ni²⁺ ions (left) and linear fitting between the ratio of 420 nm/375 nm absorption bands and upon incremental of concentration of Ni²⁺ ions

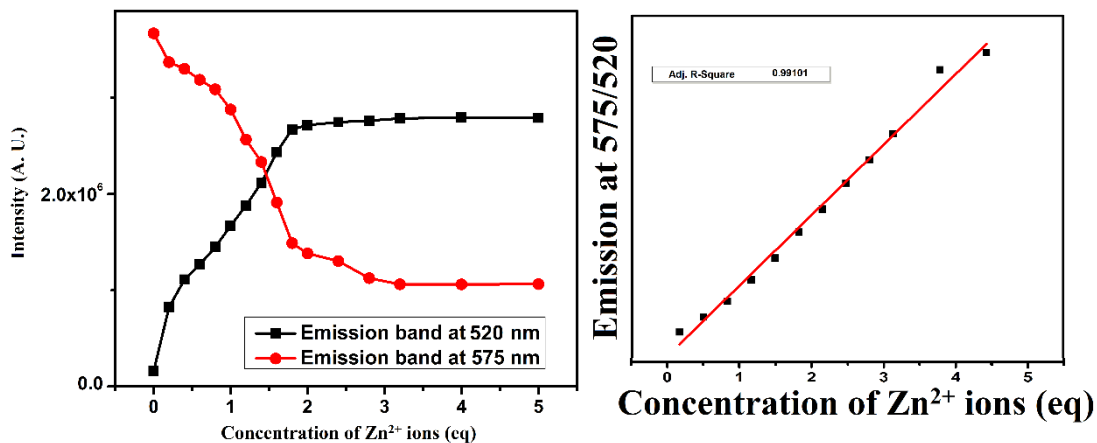


Figure S8: The compared emission bands at 375 nm and 420 nm, which indicates the ratiometric response towards Zn^{2+} ions (left) and linear fitting between the ratio of 420 nm/375 nm emission bands and upon incremental of concentration of Zn^{2+} ions

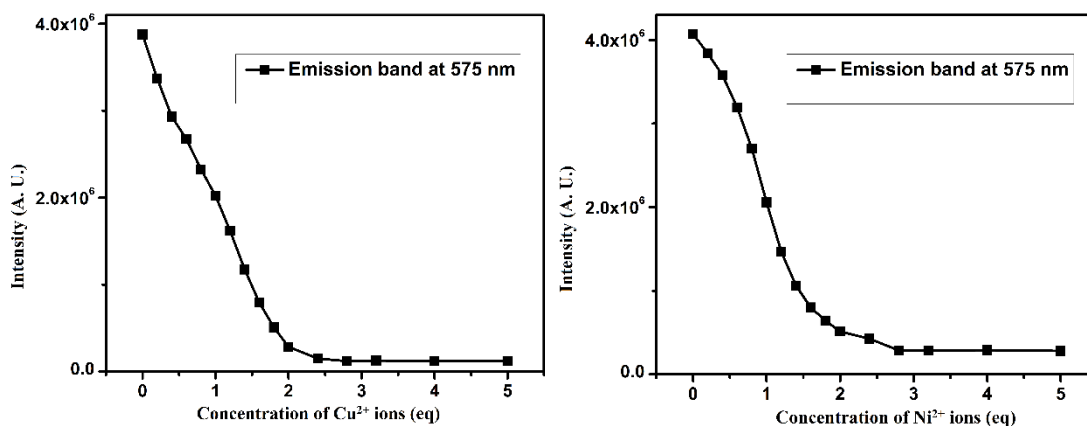


Figure S9: Change in emission spectra, upon addition of Cu^{2+} (left) and Ni^{2+} ions (right)

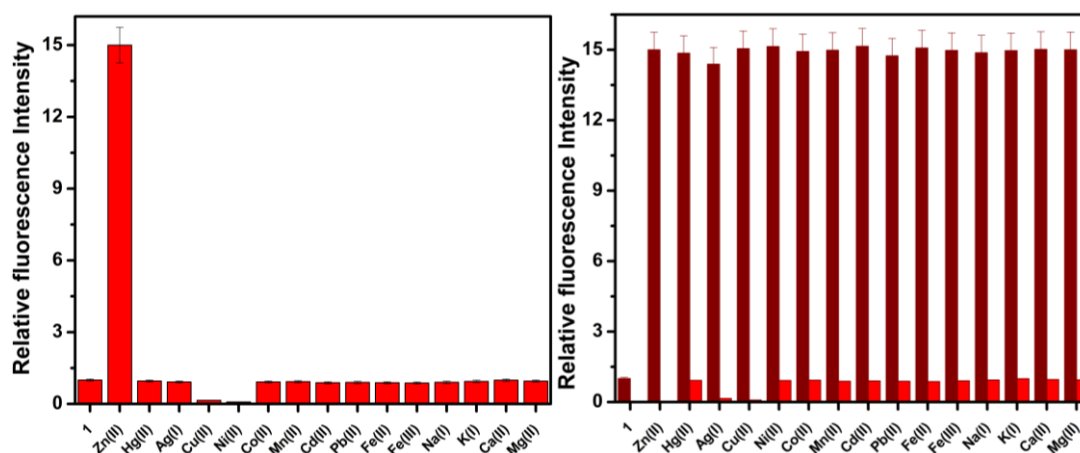


Figure S10: Examination of selectivity (left) and competitive (right) studies of **compound-1** ($1\mu M$) toward various metal ions (with error bar). The competitive binding ability of **compound-1** ($1\mu M$) were performed towards Zn^{2+} in the presence of other interfering metal ions and the emission band was monitored at 520 nm.

3. ^1H and ^{13}C Nuclear Magnetic Resonance (NMR) and High-Resolution Mass Spectroscopic (HR MS) studies

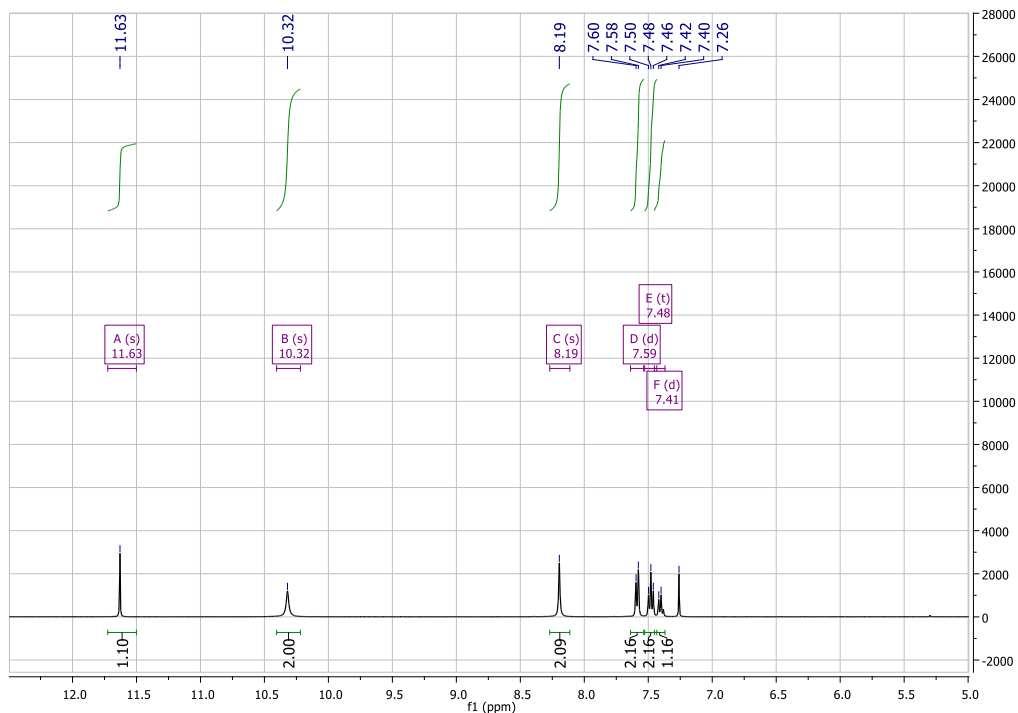
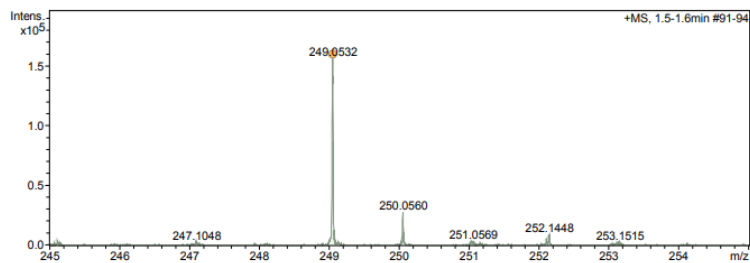


Figure S11: ^1H NMR of A (400 MHz, CDCl_3)

Compound Spectrum SmartFormula Report					
Analysis Info			Acquisition Date 27/10/2020 13:23:29		
Analysis Name	D:\Data\Keynan\K_9954_SV-Cs_RC2_01_4213.d		Operator	Larisa Panz	
Method	direct pos new.m		Instrument	maXis impact 282001.00128	
Sample Name	K_9954_SV-Cs		Comment		
Acquisition Parameter					
Source Type	ESI	Ion Polarity	Positive	Set Nebulizer	3.0 Bar
Focus	Active	Set Capillary	4500 V	Set Dry Heater	180 °C
Scan Begin	50 m/z	Set End Plate Offset	-500 V	Set Dry Gas	8.0 l/min
Scan End	3000 m/z	Set Charging Voltage	2000 V	Set Divert Valve	Source
		Set Corona	0 nA	Set APCI Heater	0 °C

+MS, 1.5-1.6min #91-94



Meas. m/z	#	Ion Formula	m/z	err [ppm]	mSigma	# mSigma	Score	rdb	e ⁻ Conf	N-Rule	err [mDa]
249.0532	1	C14H10NaO3	249.0532	-4.0	13.6	1	100.00	9.5	even	ok	1.0
	1	C14H10NaO3	249.0522	-4.0	13.6	1	100.00	9.5	even	ok	1.0

Figure S12: HRMS of A

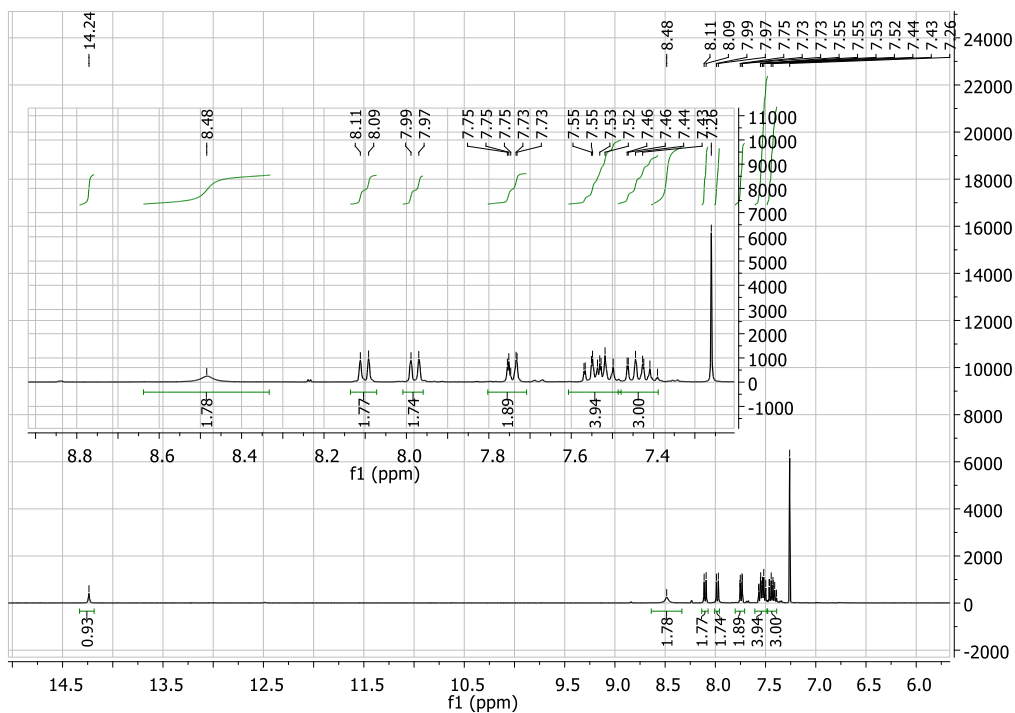


Figure S13: ^1H NMR of compound-1 (400 MHz, CDCl_3)

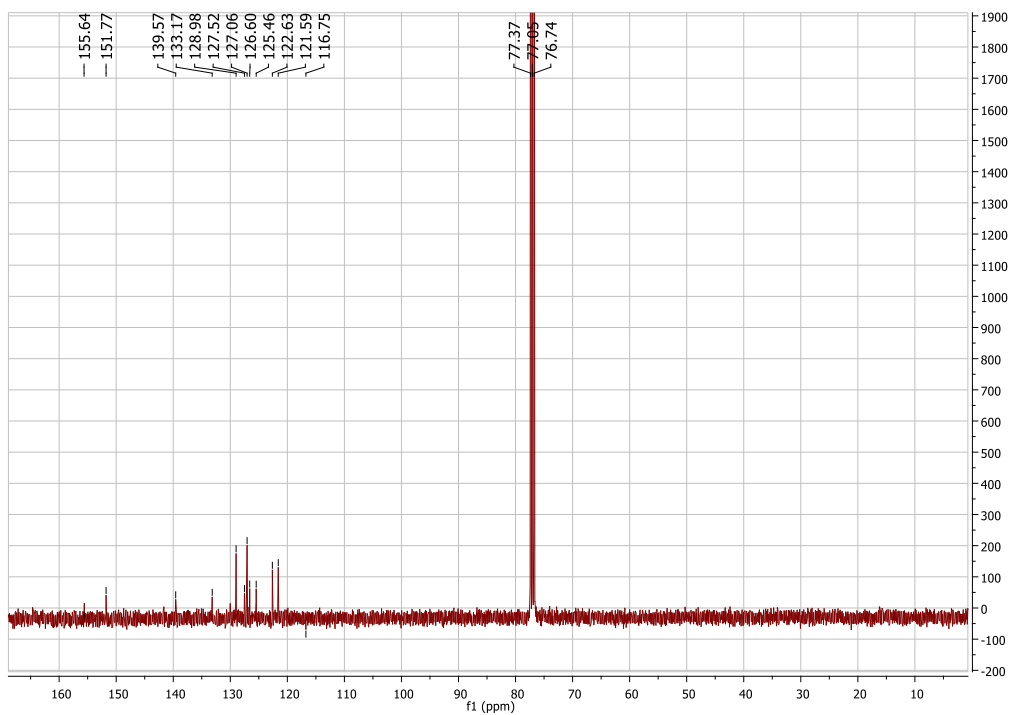


Figure S14: ^{13}C NMR of compound-1 (101 MHz, CDCl_3)

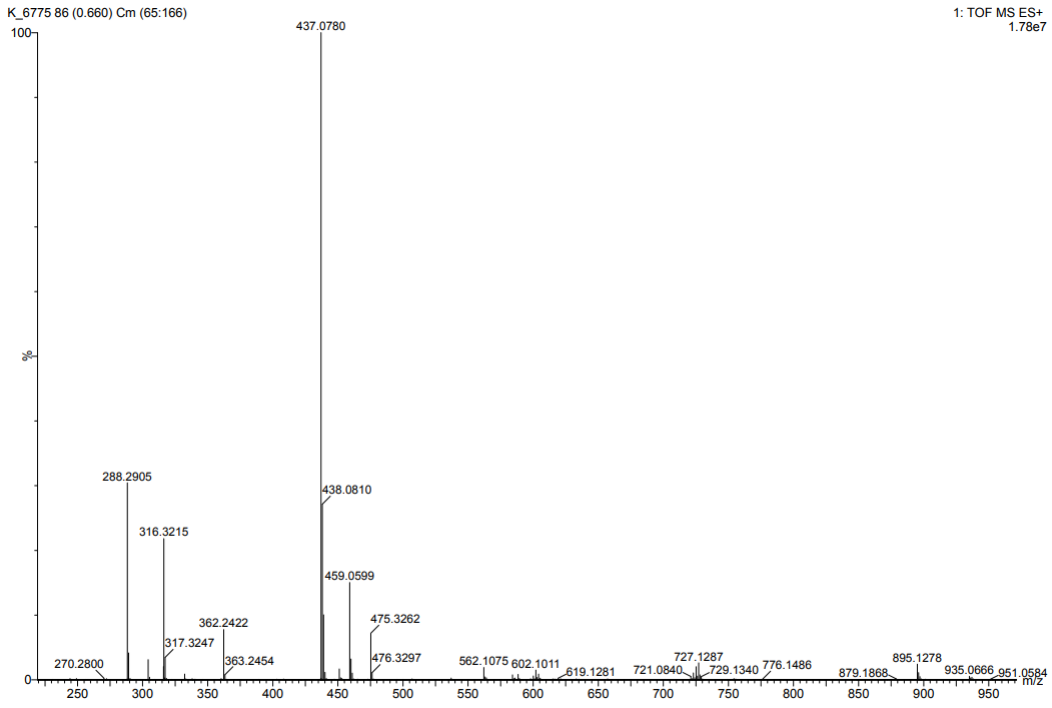


Figure S15: HRMS of compound-1

4. Density Functional Theory results

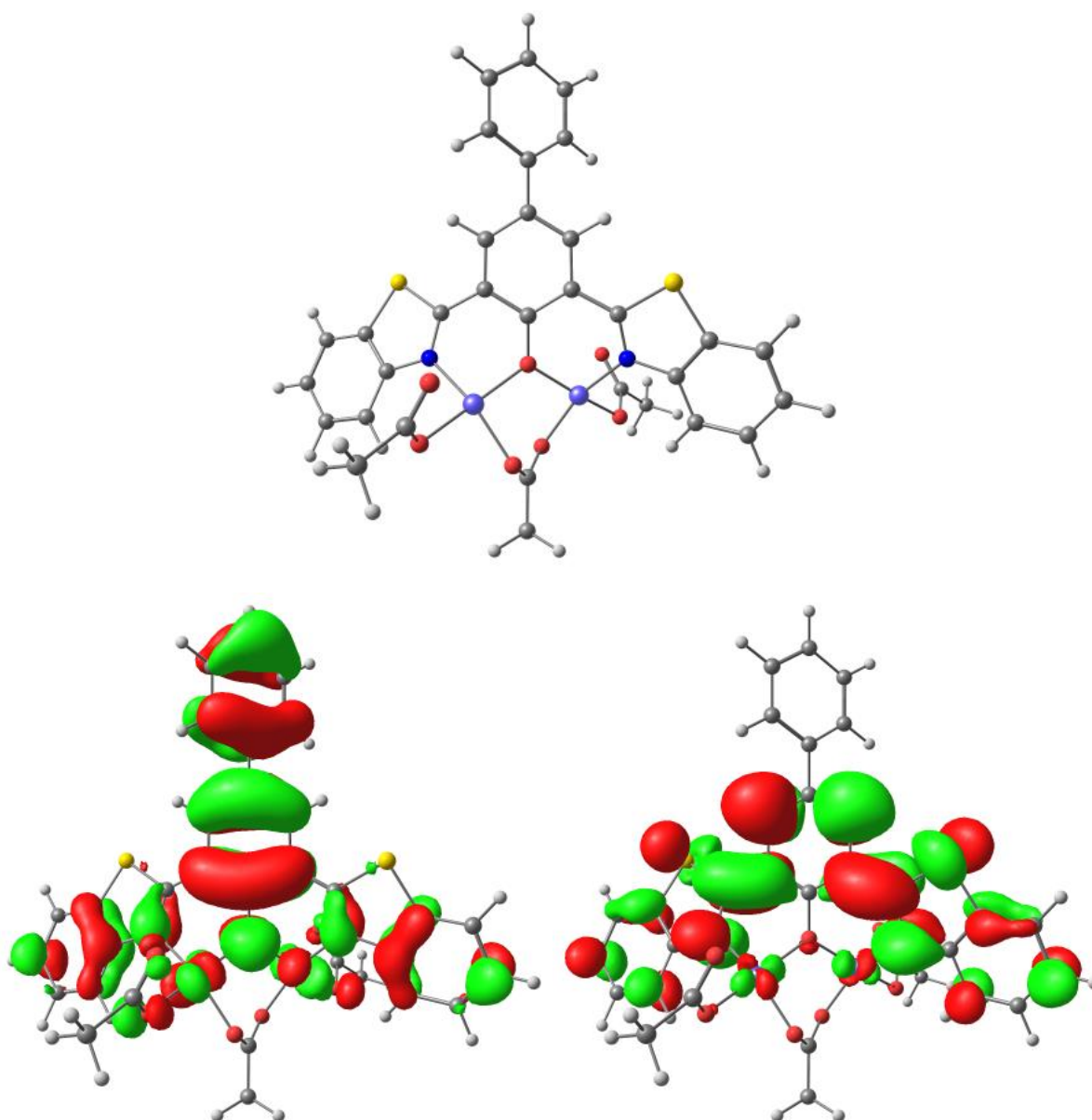


Figure S16: Density functional theory calculations of **compound-1+Ni²⁺** ions, molecular structure (top) HOMO (left) and LUMO (right)

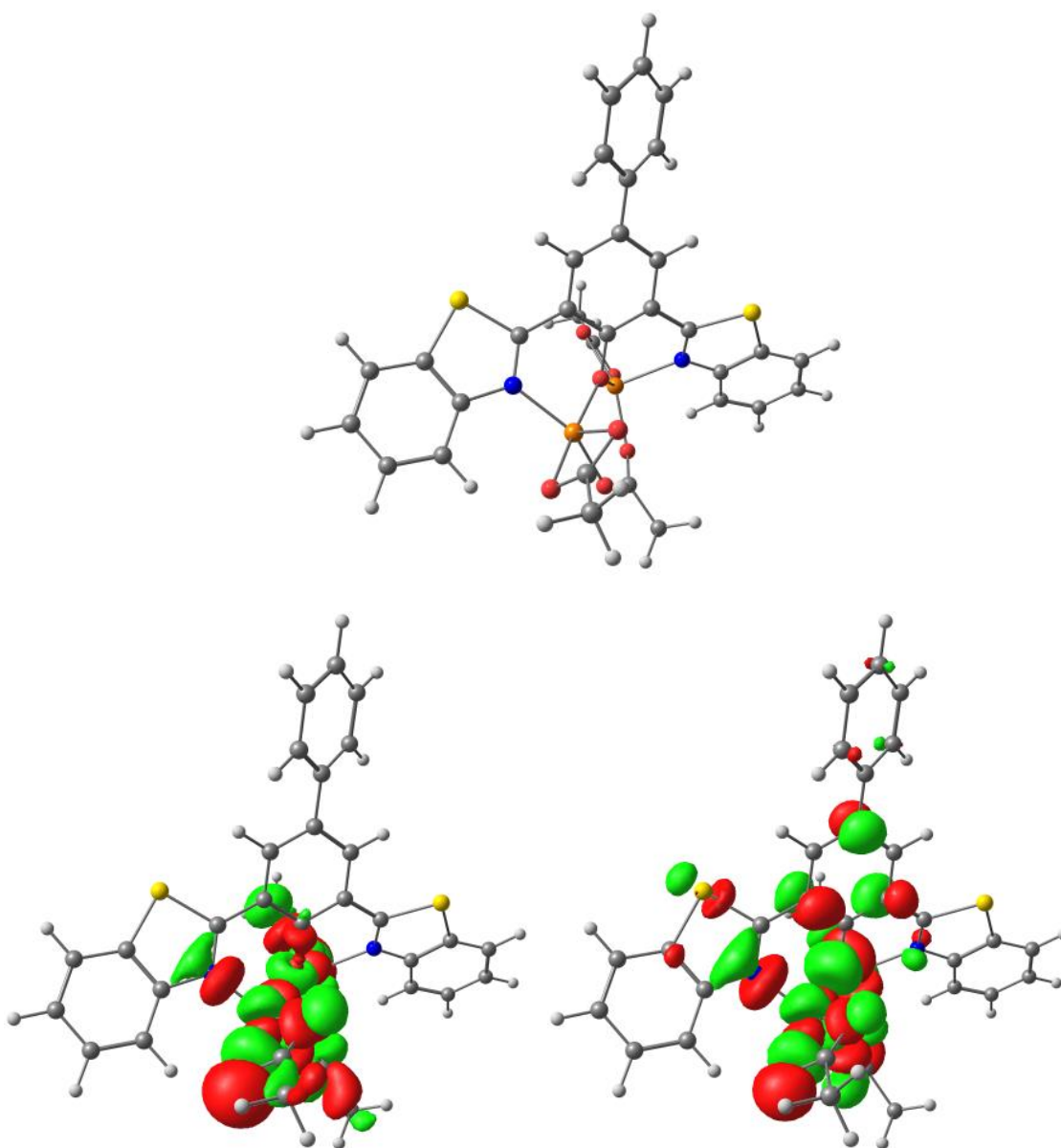


Figure S17: Density functional theory calculations of **compound-1+Ni²⁺** ions, molecular structure (top) HOMO (left) and LUMO (right)

Table-S2: Band gap of **compound-1**, **compound-1+Zn²⁺**, **compound-1+Cu²⁺** and **compound-1+Ni²⁺** ions obtained from DFT data

Compound	HOMO (eV)	LUMO (eV)	LUMO-HOMO (eV)
compound-1	-6.2353	-2.2158	4.0195
compound-1+Zn²⁺	-6.3549	-2.4654	3.8894 eV
compound-1+Cu²⁺	-5.7753	-3.4104	2.3649
compound-1+Ni²⁺	-6.4761	-2.6805	3.7955

Table S3: Selected electronic transition from TDDFT of **compound-1**

Excited State 1:	Singlet-A	3.1842 eV	389.37 nm	f=0.3326	<S**2>=0.000
113 -> 114	0.69364				
Excited State 4:	Singlet-A	4.0395 eV	306.93 nm	f=0.2015	<S**2>=0.000
110 -> 114	0.55750				
Excited State 9:	Singlet-A	4.4048 eV	281.48 nm	f=0.2330	<S**2>=0.000
111 -> 115	0.52239				
Excited State 10:	Singlet-A	4.4401 eV	279.24 nm	f=0.3185	<S**2>=0.000
113 -> 116	0.60032				

Compound-1-Zn²⁺

Excited State 1:	Singlet-A	3.0143 eV	411.32 nm	f=0.3032	<S**2>=0.000
189 -> 190	0.69776				
Excited State 3:	Singlet-A	3.8039 eV	325.94 nm	f=0.1024	<S**2>=0.000
188 -> 190	0.62059				
Excited State 8:	Singlet-A	4.0035 eV	309.69 nm	f=0.3702	<S**2>=0.000
183 -> 190	0.51814				
Excited State 9:	Singlet-A	4.1981 eV	295.33 nm	f=0.1164	<S**2>=0.000
188 -> 191	0.54358				
Excited State 16:	Singlet-A	4.4042 eV	281.51 nm	f=0.5078	<S**2>=0.000
189 -> 192	0.61891				

Compound-1+Ni

Excited State 9:	Singlet-A	2.8988 eV	427.70 nm	f=0.2085	<S**2>=0.000
187 -> 188	0.69139				
Excited State 17:	Singlet-A	3.5438 eV	349.86 nm	f=0.0647	<S**2>=0.000
184 -> 188	0.49622				
Excited State 18:	Singlet-A	3.5580 eV	348.47 nm	f=0.0253	<S**2>=0.000
187 -> 190	0.54301				

Excited State 19: Singlet-A 3.6332 eV 341.25 nm f=0.0021 <S**2>=0.000
183 -> 188 0.62797

Excited State 20: Singlet-A 3.7099 eV 334.19 nm f=0.0445 <S**2>=0.000
182 -> 188 0.37806

Compound-1+Cu

Excited State 15: Singlet-A 2.2652 eV 547.35 nm f=0.0468 <S**2>=0.000
181 -> 189 0.29469

Excited State 16: Singlet-A 2.3998 eV 516.63 nm f=0.0252 <S**2>=0.000
169 -> 189 0.32584

Excited State 17: Singlet-A 2.4664 eV 502.70 nm f=0.0090 <S**2>=0.000
188 -> 190 0.68130

Excited State 18: Singlet-A 2.5276 eV 490.52 nm f=0.0022 <S**2>=0.000
167 -> 189 0.44917

Excited State 19: Singlet-A 2.7148 eV 456.70 nm f=0.0005 <S**2>=0.000
177 -> 189 0.70509

Excited State 20: Singlet-A 2.7289 eV 454.34 nm f=0.0038 <S**2>=0.000
165 -> 189 0.36985

Table S4: Computational results of optimized structure of **Compound-1**

1	6	3.994961304	-2.231732169	-0.053181004
2	6	4.977383381	-1.203880094	0.007291001
3	6	6.347216460	-1.500002115	0.013706001
4	6	6.731137518	-2.853008215	-0.041811003
5	6	5.761300456	-3.882807298	-0.102161008
6	6	4.391482337	-3.582221275	-0.108468008
7	6	2.558159193	-0.452437034	0.009948001

8	1	7.096475564	-0.715575056	0.060383005
9	1	7.787442618	-3.108299238	-0.037855003
10	1	6.084524460	-4.919483378	-0.143864011
11	1	3.637727280	-4.362134330	-0.153758012
12	6	1.276434099	0.237616018	0.024165002
13	6	1.189584090	1.646178128	0.068954005
14	6	0.076456006	-0.550141040	-0.006842001
15	6	-0.046133004	2.312192178	0.070359005
16	1	2.105908160	2.228595170	0.125619010
17	6	-1.184401090	0.112803009	0.015690001
18	6	-1.217595093	1.517602117	0.040336003
19	1	-2.187269168	2.007975152	0.031471002
20	6	-0.127104009	3.799773292	0.113382008
21	6	-1.176634091	4.451735342	0.805016060
22	6	0.844131064	4.601267349	-0.534195040
23	6	-1.253706095	5.854425439	0.846945065
24	1	-1.920808145	3.862718296	1.335783100
25	6	0.771921061	6.004107457	-0.488756037
26	1	1.642937124	4.128435317	-1.100889083
27	6	-0.278639021	6.639136508	0.201549015
28	1	-2.065787158	6.332671494	1.389485108
29	1	1.525470114	6.598941527	-0.999630074
30	1	-0.336870026	7.724292616	0.234807018
31	6	-2.443208189	-0.650001052	0.000479000
32	6	-4.029085310	-2.201518170	0.456660035
33	6	-4.812924368	-1.436851108	-0.457939035
34	6	-4.579689348	-3.344816253	1.069457081
35	6	-6.132928462	-1.800942137	-0.765601060
36	6	-5.897843427	-3.710818284	0.762451058
37	1	-3.971339303	-3.916986301	1.762859134

38	6	-6.668366512	-2.945702225	-0.147346011
39	1	-6.731320507	-1.221054091	-1.461941110
40	1	-6.335344474	-4.591251352	1.225936095
41	1	-7.688561563	-3.245676250	-0.373446028
42	8	0.121055009	-1.906499144	-0.089856007
43	1	1.093648086	-2.217222172	-0.095291007
44	16	-3.850586293	-0.041459003	-1.089600081
45	16	4.179126317	0.425809033	0.071678006
46	7	-2.727311209	-1.723434133	0.680292052
47	7	2.671115204	-1.771321133	-0.050950004

Table S5: Computational results of optimized structure of **Compound-1+Zn²⁺** Complex

1	6	-4.121628240	-0.778462067	-0.432917262
2	6	-4.827035271	0.188608826	-1.195306099
3	6	-6.133002388	-0.043309983	-1.648990922
4	6	-6.732476601	-1.272344252	-1.320489857
5	6	-6.040526547	-2.236182402	-0.546990943
6	6	-4.736091398	-2.000630262	-0.092602844
7	6	-2.476772309	0.827115153	-0.473038951
8	1	-6.669539434	0.696454940	-2.235281213
9	1	-7.743457564	-1.480387113	-1.660741303
10	1	-6.531847514	-3.171085139	-0.292597976
11	1	-4.216197506	-2.716299099	0.534821983
12	6	-1.208911246	1.516855363	-0.221471262
13	6	-1.176941003	2.926968266	-0.224735757
14	6	0.002106125	0.777146004	-0.000494781
15	6	0.006724784	3.656670354	-0.005463226
16	1	-2.099151953	3.471550394	-0.409956261
17	6	1.215447114	1.513718929	0.217969167
18	6	1.188046846	2.923919147	0.216357822

19	1	2.111992968	3.466169190	0.399753194
20	6	0.009132012	5.146895401	-0.008017035
21	6	1.117041842	5.871221578	-0.510179257
22	6	-1.096429330	5.876503296	0.491668107
23	6	1.121221284	7.276631683	-0.510615299
24	1	1.966403078	5.336841458	-0.929551168
25	6	-1.096059965	7.281913401	0.487314037
26	1	-1.947499279	5.346284626	0.912857213
27	6	0.013730033	7.990038816	-0.012860066
28	1	1.980023042	7.812351679	-0.907914169
29	1	-1.953113320	7.821762567	0.882795183
30	1	0.015491135	9.077212836	-0.014701073
31	6	2.481000435	0.820704171	0.472181155
32	6	4.121028153	-0.789931984	0.437542271
33	6	4.828995344	0.177348992	1.197287339
34	6	4.732227346	-2.014801100	0.101059096
35	6	6.134036400	-0.057013028	1.652369189
36	6	6.035726380	-2.252805976	0.556825173
37	1	4.210796194	-2.730573126	-0.524933777
38	6	6.730082603	-1.288768327	1.327898338
39	1	6.672400695	0.682942928	2.236738038
40	1	6.524472370	-3.189853998	0.305378136
41	1	7.740240695	-1.498792956	1.669369009
42	8	0.000031751	-0.570510226	0.001839949
43	16	3.803510161	1.648980868	1.443967018
44	16	-3.797231473	1.656371886	-1.446965865
45	7	2.817384125	-0.394984249	0.068207243
46	7	-2.816793034	-0.386215782	-0.065178233
47	30	1.474247069	-1.599366267	-1.027498173
48	30	-1.477866112	-1.589738945	1.036070844

49	8	1.038392874	-3.450693402	-0.452115283
50	6	-0.009444226	-4.056120330	0.004351954
51	8	-1.052327169	-3.443360063	0.462518908
52	6	-0.028451215	-5.571686617	-0.024379196
53	1	-0.483664831	-5.901503217	-0.967758295
54	1	0.990685957	-5.963075635	0.019268931
55	1	-0.633581804	-5.957704486	0.799763039
56	8	3.010674052	-2.152686170	-2.597378154
57	6	2.213120328	-1.594282990	-3.452057092
58	8	1.095167243	-1.063493867	-3.000929253
59	6	2.519543060	-1.554780967	-4.929170185
60	1	1.861331231	-2.260701301	-5.451869246
61	1	2.312315133	-0.555964201	-5.327143227
62	1	3.560005017	-1.831886221	-5.112602599
63	8	-3.014004165	-2.132103291	2.610214407
64	6	-2.217365917	-1.565283019	3.460196367
65	8	-1.099789077	-1.037392200	3.004727158
66	6	-2.524735347	-1.511277305	4.936634230
67	1	-3.558761450	-1.808566967	5.124491624
68	1	-1.849906294	-2.193031172	5.469907311
69	1	-2.340690146	-0.501802910	5.319236260

Table S6: Computational results of optimized structure of **Compound-1+Cu²⁺** Complex

1	6	-4.132728262	-0.570840961	-0.224804021
2	6	-4.787656546	0.360659167	-1.077563103
3	6	-6.116187251	0.168637147	-1.483590223
4	6	-6.786390766	-0.976837918	-1.016621993
5	6	-6.141315233	-1.905690043	-0.162193885
6	6	-4.813494155	-1.713420369	0.241961005
7	6	-2.390023224	0.887438184	-0.445769919

8	1	-6.618479650	0.875935988	-2.136503400
9	1	-7.816838573	-1.149276145	-1.316662847
10	1	-6.685572446	-2.779270133	0.185879859
11	1	-4.301819443	-2.409763123	0.898439250
12	6	-1.064179152	1.487285996	-0.264110248
13	6	-0.916654060	2.884736217	-0.348834172
14	6	0.081776935	0.677765987	0.024532128
15	6	0.322467915	3.529661464	-0.157150826
16	1	-1.791330077	3.486951039	-0.578769095
17	6	1.343632895	1.323616236	0.225917939
18	6	1.441651338	2.722883122	0.132353051
19	1	2.407954395	3.194274216	0.290035171
20	6	0.444589853	5.009378639	-0.258541187
21	6	1.620062389	5.607897158	-0.773992107
22	6	-0.612032118	5.855668529	0.157511196
23	6	1.736051163	7.004858419	-0.869028108
24	1	2.432874939	4.981739182	-1.133859095
25	6	-0.497786984	7.252651486	0.061299893
26	1	-1.513311992	5.424532478	0.586615206
27	6	0.677433135	7.834943314	-0.451981930
28	1	2.643467376	7.443251606	-1.277019004
29	1	-1.317718026	7.884220829	0.394327011
30	1	0.766367192	8.915879922	-0.526248782
31	6	2.530600219	0.519239829	0.509495030
32	6	3.964879059	-1.273385144	0.514441779
33	6	4.753249442	-0.396581835	1.306316903
34	6	4.435913487	-2.563868005	0.199087065
35	6	6.002663385	-0.784821190	1.810075122
36	6	5.681914238	-2.955600989	0.705725067
37	1	3.853065494	-3.204286249	-0.453140299

38	6	6.457419263	-2.079993091	1.505329353
39	1	6.602679476	-0.114145120	2.417583304
40	1	6.063036689	-3.946192223	0.473939082
41	1	7.420719768	-2.409719201	1.885456951
42	8	-0.009794013	-0.680709271	0.112041111
43	16	3.901637086	1.189530130	1.523670107
44	16	-3.665105440	1.719044994	-1.499795217
45	7	2.736883036	-0.718098819	0.100815145
46	7	-2.807162008	-0.234030226	0.094321082
47	29	1.302060201	-1.729340137	-0.931982208
48	29	-1.423308996	-1.448315267	1.293230349
49	8	0.148081257	-3.328513254	-1.132901285
50	6	-1.018359282	-3.676351514	-0.690447191
51	8	-1.586271247	-3.180266365	0.363092853
52	6	-1.765732186	-4.753571181	-1.456475180
53	1	-2.429470213	-4.278180566	-2.191103909
54	1	-1.058886321	-5.392899321	-1.992013140
55	1	-2.380418128	-5.343439240	-0.770245003
56	8	2.631244440	-2.491924241	-2.300444099
57	6	2.329756286	-1.643599135	-3.267578494
58	8	1.471894347	-0.711632273	-3.035826376
59	6	2.991326274	-1.822729338	-4.615343205
60	1	2.577753087	-2.714086080	-5.104196618
61	1	2.806178267	-0.948511060	-5.244747154
62	1	4.068039518	-1.982205369	-4.490821448
63	8	-2.616712174	-1.859892927	3.095786392
64	6	-1.975054067	-0.881297082	3.652863453
65	8	-1.063837303	-0.271553126	2.922303039
66	6	-2.216947338	-0.458810963	5.077659437
67	1	-3.194207010	-0.812189179	5.417063671

68	1	-1.441797920	-0.896718895	5.720213441
69	1	-2.150529243	0.630212003	5.165947370

Table S7: Computational results of optimized structure of **Compound-1+Ni²⁺** Complex

1	6	4.040978452	-0.838231050	0.556081150
2	6	4.776523186	0.181815248	1.212105889
3	6	6.055396427	-0.041165227	1.740807937
4	6	6.599615540	-1.330258998	1.618251015
5	6	5.870985565	-2.360938055	0.977703123
6	6	4.597113578	-2.129711410	0.441907983
7	6	2.475344060	0.843811224	0.400443241
8	1	6.606280527	0.750886112	2.238899198
9	1	7.586951805	-1.536093073	2.022809139
10	1	6.308015592	-3.352268021	0.894436024
11	1	4.054095168	-2.901783133	-0.086827932
12	6	1.211952957	1.523794993	0.148148992
13	6	1.187293297	2.934084112	0.138441235
14	6	-0.003043828	0.784744989	-0.004224951
15	6	-0.001798144	3.669307107	-0.001827778
16	1	2.122554288	3.473252228	0.261549030
17	6	-1.218107289	1.524830064	-0.149898981
18	6	-1.191810883	2.935277407	-0.139713906
19	1	-2.126763364	3.475580079	-0.260017062
20	6	-0.000721798	5.158683354	-0.003156013
21	6	-1.064687162	5.885215670	0.582785021
22	6	1.064521000	5.882094583	-0.590656003
23	6	-1.064969214	7.290589791	0.579823216
24	1	-1.878845410	5.353480378	1.069981051
25	6	1.067275897	7.287469762	-0.590724267
26	1	1.877697095	5.347809186	-1.076698957

27	6	0.001774860	7.999083513	-0.006219949
28	1	-1.887991181	7.829902372	1.042370170
29	1	1.891247208	7.824319552	-1.054441232
30	1	0.002717854	9.086229487	-0.007397898
31	6	-2.484475013	0.846519024	-0.391498029
32	6	-4.056552138	-0.831334812	-0.529669913
33	6	-4.797008167	0.191307101	-1.176140887
34	6	-4.615134180	-2.121337180	-0.410228258
35	6	-6.082663344	-0.027455832	-1.689875156
36	6	-5.895975431	-2.348312944	-0.931050856
37	1	-4.067876532	-2.895577472	0.110891209
38	6	-6.629229357	-1.315031923	-1.561962961
39	1	-6.636992387	0.766663002	-2.180800299
40	1	-6.334679246	-3.338548042	-0.843638183
41	1	-7.621889675	-1.517616849	-1.954964911
42	8	-0.002718913	-0.580282013	-0.009976049
43	16	-3.833955316	1.718712141	-1.256637213
44	16	3.816702550	1.711942906	1.281951994
45	7	-2.771518216	-0.410481205	-0.094069194
46	7	2.762717998	-0.413477935	0.105632775
47	28	-1.479993934	-1.574474298	0.731850019
48	28	1.482879008	-1.566529231	-0.750088113
49	8	-0.408324807	-3.150879035	1.028421058
50	6	-0.014913802	-3.757333096	-0.056829932
51	8	0.409718131	-3.125005443	-1.114060987
52	6	-0.029712773	-5.268832656	-0.078494978
53	1	0.848274834	-5.639037651	0.467540800
54	1	-0.922803100	-5.644022501	0.429399291
55	1	0.020907264	-5.630565523	-1.107900835
56	8	-2.787550170	-2.404326356	1.778500174

57	6	-2.947414087	-1.739670206	2.937161278
58	8	-2.346696308	-0.657325987	3.186749315
59	6	-3.899071106	-2.412543420	3.910730468
60	1	-3.477984131	-3.375077148	4.225862399
61	1	-4.048157271	-1.773411077	4.784386231
62	1	-4.859671220	-2.614583294	3.422733263
63	8	2.808130402	-2.384237200	-1.783512012
64	6	2.999523229	-1.702494975	-2.927316465
65	8	2.413761057	-0.611433090	-3.173972331
66	6	3.967422285	-2.368752415	-3.889564437
67	1	4.910195476	-2.599015429	-3.379970450
68	1	3.539109395	-3.316178133	-4.239074368
69	1	4.151366414	-1.712441920	-4.743637466